

Evaluation of Tissue-engineered Skin on Base of Human Amniotic Membrane for Wound Healing

Samuel John, MD
 Marco Rainer Kesting, MD Prof
 Mechthild Stoeckelhuber, Prof
 Achim von Bomhard, MD

Background: Human amniotic membranes (hAMs) have shown promising results in recent studies aimed at improving wound healing through several mechanisms. We wanted to investigate its properties as a scaffold by adding autologous cells to treat full-thickness skin defects and hypothesized that recultivated hAM would show an even improved wound healing by accelerating the epidermal closure of the wound.

Methods: In an air–liquid cell culture, we cultivated autologous keratinocytes and fibroblasts on the hAM until a mostly keratinized surface was achieved. These hAM, de-epithelialized hAM, native hAM with remaining allogeneous cells, and negative controls were compared in the treatment of circular 30×30 mm² full-thickness skin defects in 4 groups of 6 rats with one wound each. We evaluated the wound contraction every 10 days until wound closure, the macroscopic scar appearance on the Vancouver Scar Scale and the qualitative histological properties of the scar regarding morphology and continuity of the basement membrane.

Results: Rats treated with de-epithelialized hAM showed more extent wound contraction ($P < 0.001$) than the other 3 groups, which did not differ significantly compared with the control group ($P > 0.05$). Vancouver Scar Scale showed no significant statistical differences between the 4 groups ($P = 0.46$). The scar structure of all rats showed similar morphologies, the only difference being the absence of a basement membrane in the negative controls compared with the groups treated with hAM.

Conclusion: The rats treated with hAM showed no improved wound healing but a tendency toward a more prominent basement membrane in the resulting scar. (*Plast Reconstr Surg Glob Open* 2019;7:e2320; doi: 10.1097/GOX.0000000000002320; Published online 25 July 2019.)

INTRODUCTION

The skin acts as an important barrier against noxious agents and helps to maintain a stable water balance.¹ Various pathologies such as burn injuries, tumor resections, and chronic wounds are often responsible for large skin defects, which need to be covered properly and in a timely manner.^{2–5} Nowadays, diverse autologous and allogeneous grafts are used to cover such defects, although limitations often include restricted availability, secondary defects, rejection of the graft, or both functional and aesthetical

problems of the resulting scar.^{6–9} A promising scaffold for tissue-engineered skin and one that targets the limitation of other grafts is the human amniotic membrane (hAM). It provides a stable basement membrane for cell culturing, expresses anti-immunogenic and anti-inflammatory agents, and shows good results in the treatment of wound defects, such as a wound coverage.^{10–14}

As skin usually shows an orthokeratinized surface, various studies have proposed air–liquid interface cultures to reproduce its typical morphology.¹⁵ This method allows air to come into contact with the surface as the typical stimulus for the keratinocytes to differentiate into corneocytes, while providing nutrients from the dermal site of the graft. Such engineered skin might also improve wound healing by providing not only a basement membrane, which plays an important role not only in the re-epithelialization but also in the structuring and vascularization of the dermis, but also autologous skin cells that can be incorporated into the final scar.^{16–18} After the development of an air–liquid model on the base of hAM in a previous

Received for publication April 19, 2019; accepted April 30, 2019.

This work was supported by internal financial sources of the Technical University.

Copyright © 2019 The Authors. Published by Wolters Kluwer Health, Inc. on behalf of The American Society of Plastic Surgeons. This is an open-access article distributed under the terms of the Creative Commons Attribution-Non Commercial-No Derivatives License 4.0 (CCBY-NC-ND), where it is permissible to download and share the work provided it is properly cited. The work cannot be changed in any way or used commercially without permission from the journal.

DOI: 10.1097/GOX.0000000000002320

Disclosure: The authors have no financial interest to declare in relation to the content of this article.

study, we now compared autologous recultivated hAM, de-epithelialized hAM, native hAM, and a control group in a rat model with regard to macroscopic and microscopic outcomes of wound healing.¹⁹ The question we wanted to answer is: does differently processed hAM have an advantage over a control group in the treatment of full-thickness skin defects?

MATERIAL AND METHODS

Preparation of hAM

The cryoconserved hAMs were prepared as described in recent research.¹⁹ They were gently thawed at room temperature, rinsed thoroughly in Dulbecco's Phosphate-Buffered Saline (DPBS), cut into smaller pieces of $5 \times 5 \text{ cm}^2$ and transferred for de-epithelialization. As previously reported by a similar research group, we used Trypsin and a cell scraper.²⁰ The thawed hAM was transferred into 0.25/0.02% Trypsin/Ethylenediaminetetraacetic acid (EDTA) at 37°C and incubated for 25 minutes. Cold DPBS⁺ was used to stop enzyme activity. Under phase contrast microscopy, the epithelium was removed by slow and gentle scraping with a cell scraper. The hAM was then placed on an insert in a well and fixed with a Polytetrafluoroethylene (PTFE) ring with the epithelial side pointing up. Following the de-epithelialization step, a further rinse in DPBS⁺ and Aprotinin (10 KIU/ml) on a shaker was carried out at 4°C for 48 hours with a regular medium change to remove loose epithelial cells and enzyme residues.

Cell Isolation and Cultures

Rat skin obtained through biopsies (see below) was used to isolate keratinocytes and fibroblasts, which subsequently were amplified and cultured on the de-epithelialized hAM until a confluent cell population was reached. The culture was then changed to air-liquid interface culture until final keratinization.

Isolation of the Keratinocytes

The isolation of fibroblasts and keratinocytes was performed by means of the protocol for the isolation of various cell lines from corneal tissue.²¹ The sample was stored in serum-free keratinocyte medium for up to 4 hours. After removal of the subcutis, the tissue was cut into pieces of 5 mm, which were then incubated in Thermolysin (50 IU/ml) for 15 hours at 4°C. Enzyme activity was subsequently stopped with keratinocyte medium. Sterile forceps were used to remove the epidermal layer, which was cut into smaller pieces. These were transferred into centrifuge tubes filled with TrypLE and, by occasional gentle shaking, the cells were dissociated over the course of 30 minutes at 37°C. Subsequently, the dissociation was stopped with cold keratinocyte medium and the cell suspension was filtered through a cell strainer and centrifuged. The remaining cell pellet was resuspended in keratinocyte medium and transferred to cell culture flasks ($20 \times 10^3/\text{cm}^2$).

Isolation of the Fibroblasts

After removal of the epidermis, the remaining pieces of dermis were transferred to fibroblast medium and cut into smaller pieces, which were then placed in a cell culture dish. After 4 hours, the dish was filled with fibroblast medium. Several days later and after regular medium changes, the pieces were removed once fibroblast colonies had become visible.

Medium Changes and Cell Passages

To amplify the cells, regular medium changes and cell passages had to be performed. The medium was changed every second or third day for keratinocytes or fibroblasts, respectively. For a medium change, the remaining medium was removed, the flask/dish was rinsed with DPBS⁺ and new medium was administered. To passage the cells, a small amount of TrypLE was used for 15–40 minutes at 37°C. Dissociation was observed under phase contrast microscopy and, once almost all cells had detached, the enzyme was blocked with cold keratinocyte or fibroblast medium. The solution was then centrifuged and the cell pellet was resuspended in keratinocyte or fibroblast medium and recultured in cell culture flasks (keratinocytes $10 \times 10^3/\text{cm}^2$; fibroblasts $4 \times 10^3/\text{cm}^2$).

Cell Culturing on the hAM and Air-Liquid Interface Culture

An air-liquid interface culture was developed based on a published model.²² De-epithelialized hAM was placed upside down with the chorion side facing up. Then, 1 ml of fibroblast medium with around 100,000 fibroblasts was pipetted onto this side, with surface tension preventing run-off. After an incubation time of 6 hours, the insert was placed in a well with the epithelial side facing up and 1.5 ml of fibroblast medium was pipetted onto the basolateral side. Subsequently, 0.5 ml of keratinocyte medium with 500,000 keratinocytes was placed onto the epithelial side. Medium changes were performed daily. When the confluence of both cell lines had been achieved, the culture was lifted to the air-liquid interface and cultured only in keratinocyte medium with 5% FCS on the basolateral side of the insert. Regular medium changes were carried out until final keratinization was accomplished.

In Vivo Comparison in Rats

Three test groups were compared with a negative control (Fig. 1). The test groups included native hAM, de-epithelialized hAM, and de-epithelialized hAM with autologous recultivation of keratinocytes and fibroblasts. A comparison was made with regular clinical wound examination and histological analysis. The rats (Wistar-rats, Charles River Laboratories, Massachusetts, USA) were kept in accordance with the law on animal welfare (AZ 211-2531-103/13 Government of Upper Bavaria) with free access to food and water.

General Operative Preparations

At least one intervention was performed in each rat: the setting of the full skin thickness defect, possibly with membrane transplantation. Additionally, 6 of the rats

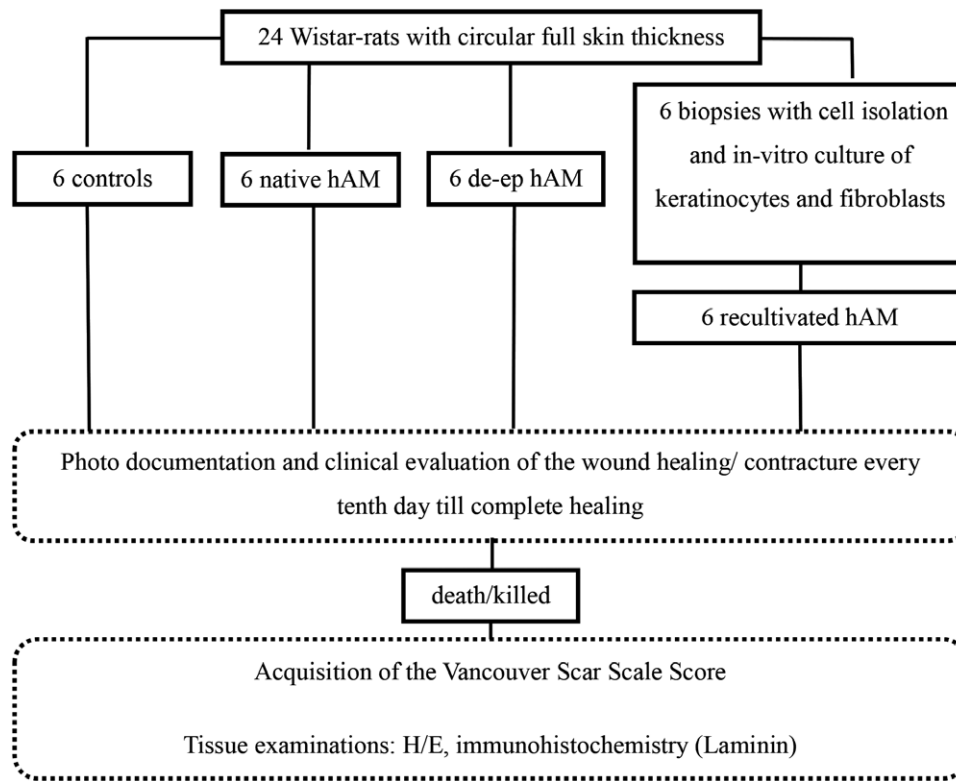


Fig. 1. Overview of the in vivo experiments. Clinical and histological comparison of differently processed hAM to cover full-thickness skin defects.

underwent a previous biopsy so that we could isolate the cells for the later recultivation of the hAM. Preoperatively, the rats were shaved and placed on a heating mat at 37°C under sterile conditions. They then received meloxicam (1 mg/kg) for pain reduction. Anesthesia was initiated by the use of medetomidine (0.15 mg/kg), midazolam (2 mg/kg), and fentanyl (0.005 mg/kg) i.p. In addition, the rats received 2 l oxygen per minute. Narcosis was antagonized with flumazenil (0.2 mg/kg), atipamezole (0.75 mg/kg), and naloxone (0.12 mg/kg). Postoperatively, the rats received meloxicam (0.5 mg/kg) for 3 days and Baytril (10 mg/kg).

Extraction of Biopsy Material and hAM Transplantation

In the first intervention, a small skin spindle (10×20 mm²) was taken and the wound was primary closed (Fig. 2). Subsequently, the cell isolation and the recultivation of the hAM were performed as described above. A circular skin defect of the size 30×30 mm² was then made in the neck of each rat (Fig. 2). Four lines of 40 mm each forming a square were tattooed around the skin defect to evaluate wound contraction (Fig. 2). The skin defect was then covered with native, de-epithelialized, or recultivated hAM (Fig. 2). The negative control group received no coverage. To protect the wound against external influences, hematoma formation, and desiccation in all rats, a dressing consisting of Jelonet and Paladur with a polymerized gauze ball was fixed over the wound (Fig. 3).

Postoperative Examination

Postoperatively, the rats were evaluated daily within a strain table until complete wound closure. After 10 days, the wound dressing was removed with subsequent regular clinical evaluation of the wound healing (Fig. 3). Concomitantly, the shrinkage of the surrounding tissue was measured and noticeable morphological characteristics of the wound were documented. The shrinkage was measured by obtaining the width and length and the 2 diagonals of the tattooed square. The measurements were then added up and the mean value for every test group was obtained. Subsequently, the data were tested for normality by using histograms and then illustrated as the mean ± SD. Intergroup comparisons were performed by using the *t*-test. Analysis was carried out with the software SPSS 16.0, with the significance level being set at 0.05. After complete wound closure, the scars were evaluated by one investigator by the Vancouver Scar Scale (VSS) in a blinded order and intergroup differences were analyzed by ANOVA (significance level 0.05).²³ Subsequently, the rats were killed, and the wound bed was extracted and histologically examined.

Tissue Examination

Hematoxylin and Eosin Staining and Immunohistochemistry

The tissue was fixed in formalin and then, over the course of 48 hours, embedded in paraffin. It was subsequently stained with hematoxylin–eosin by using an established protocol.²⁴ For immunohistochemical analysis for laminin to evaluate the consistency of the basement membrane, the 5-µm-thick sections were mounted on

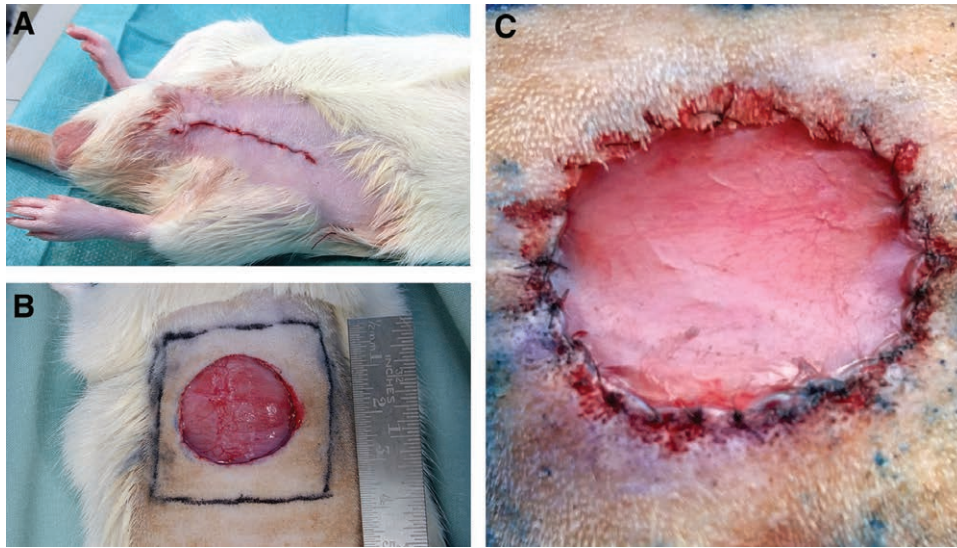


Fig. 2. Operative treatment and postoperative controls of the rats. A, Surgical site in the groin area after extraction of biopsy material. The resulting skin defect was closed per intracutaneous sutures. B, Tattooed $4 \times 4 \text{ cm}^2$ on the back of the rat. Inside of the square a round full-thickness skin defect with the diameter of the insert used to hold the hAM was created. C, Surgical site after coverage of the skin defect with hAM which was fixed with single button sutures.



Fig. 3. Operative treatment and postoperative controls of the rats. A and B, To protect the wound bed against mechanical strain, a wound dressing of jelonet, Paladur and a gauze pad was used, which was removed after 10 days. C, Typical view of a postoperative control with measurement of the wound extent and shrinkage as well as clinical evaluation of the healing process.

slides and deparaffinized by using xylene and ethanol. After treatment of the slides with a peroxide and a protein block, they were incubated with the primary antibody (polyclonal rabbit antibody against laminin) for 30 minutes and subsequently with a secondary (antirabbit antibody) for 45 minutes. The slides were then treated with streptavidin (Sigma-Aldrich, Wilmington, Missouri, USA) and counter stained with hematoxylin.

The wound biopsies were investigated qualitatively by one of the main investigators with blinding. With regards to existing histological scores the following aspects were assessed: wound re-epithelialization and complete keratinization, presence of inflammatory cells, presence of vessels, amount of granulation tissue, and collagen fiber orientation.²⁵ Additionally, the consistency of the basement membrane was evaluated.

RESULTS

In Vitro Preparations of the hAM

Treatment with trypsin and a cell scraper resulted in complete de-epithelialization of the hAM. With the protocols de-

scribed above, the culturing of keratinocytes and fibroblasts on the de-epithelialized hAM in the air-liquid culture was successful, giving a mostly keratinized surface. Few membranes had to be discarded because of detected defects that had occurred during or after de-epithelialization.

Operations and Wound Examination

The rats weighed between 420 and 650 g (mean 525 g). No rat had to be excluded or prematurely killed. The implantation of the hAM went smoothly without discharge and the membranes always adhered well to the wound bed. Wound examinations took place at regular intervals and were mainly uneventful without clinically visible wound infections. Overall, the dressing seemed to withstand the manipulation caused by the rats. However, removal of the dressing occasionally reopened the wound traumatically. The wounds and scars showed heterogeneous forms with round, linear, or angular shapes throughout all groups (Fig. 4). A craniocaudal wound contraction most commonly resulted in a transverse scar. All wounds were closed at the wound examination at day 40 while no wound was completely closed on day 30.

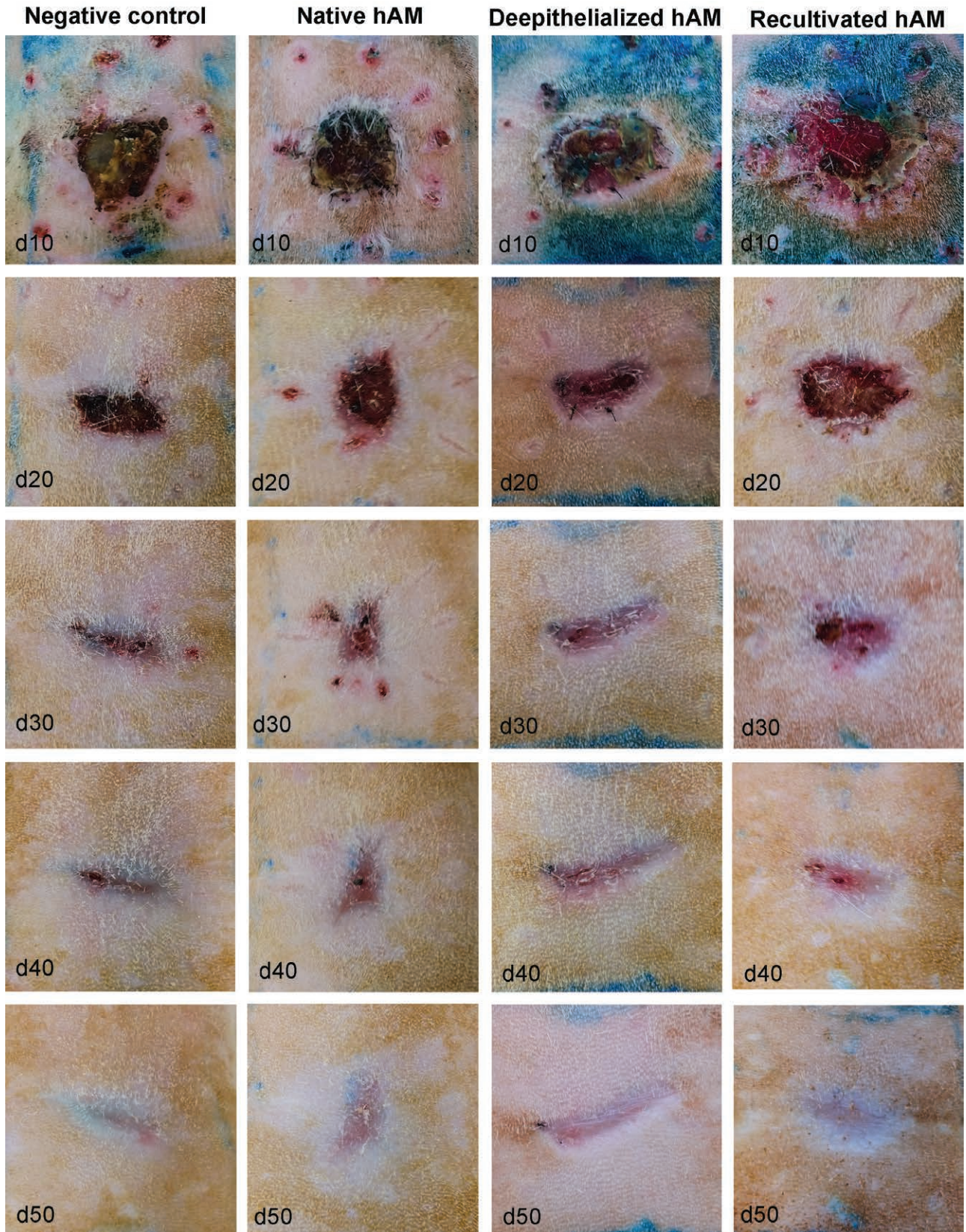


Fig. 4. Examples of wound appearances of the various groups. Left: Top down: wound appearance examined every ten days in a rat without hAM (control). Center-left: Top down: wound appearance examined every ten days with native hAM. Center-right: Top down: wound appearance examined every 10 days with de-epithelialized hAM. Right: Top down: wound appearance examined every ten days with recultivated hAM.

Table 1. t-Test of the Shrinkage Data

	Control Group	Recultivated hAM	Native hAM	De-epithelialized hAM
d10	0.97±0.03	0.94±0.07 <i>P</i> = 0.34	1.00±0.05 <i>P</i> = 0.25	0.86±0.06 <i>P</i> < 0.001*
d20	0.91±0.05	0.93±0.07 <i>P</i> = 0.47	0.91±0.05 <i>P</i> = 0.78	0.86±0.05 <i>P</i> = 0.12
d30	0.91±0.06	0.94±0.04 <i>P</i> = 0.41	0.94±0.04 <i>P</i> = 0.44	0.84±0.06 <i>P</i> = 0.06
d40	0.94±0.04	0.93±0.04 <i>P</i> = 0.64	0.96±0.05 <i>P</i> = 0.54	0.84±0.06 <i>P</i> < 0.01*

*Significant (*P* < 0.05).
Only the de-epithelialized membranes showed significant differences at d10 and d40 compared with the control group; contraction was always strongest in the de-epithelialized group.

Wound Contraction

Within the separate groups, the wound sizes and contractions that were measured and related to the initial size differed widely resulting in large variances (Table 1, Fig. 5). Although the control group and the rats treated with native and recultivated hAM showed similar mean values over the course of time, the wounds treated with de-epithelialized membranes displayed more extensive wound contraction compared with the control group; this was significant at days 10 and 40 (*P* < 0.01). When compared with the control group, no other significant deviations were found.

Vancouver Scar Scale

After complete wound closure, the scar was evaluated by VSS. As the differences between the groups regarding the mean values were only slight, a univariate ANOVA was performed to find significant differences (Table 2). A low deviation among the groups was calculated (*P* = 0.46) and therefore no further *t*-tests were performed. No signifi-

cant differences were found, even in the subcategories of the VSS.

Histological Analysis of the Wound Area

Hematoxylin–eosin staining showed no obvious differences of the scar structure between the groups; qualitatively, wound re-epithelialization and keratinization were complete in all biopsies. No intensified vascularization or increased immigration of inflammatory cells was seen when comparing groups. In addition, no differences regarding the orientation of the collagenous matrix with all groups showing mainly horizontal fibers could be found. No skin appendages and a dense connective tissue were found in the scar area in all rats (Fig. 6). Furthermore, the biopsies were analyzed with regard to their basement membranes (Fig. 7). Noticeably, in the biopsies of the rats treated with hAM, a consistent basement membrane was always found, which was especially pronounced when de-epithelialized hAM was used. In contrast, in the control group, qualitatively no basement membranes could be detected.

DISCUSSION

The in vivo experiments went mainly successful without discharge or relevant wound infections. These aspects emphasize the feasibility of hAM as a wound coverage material, as previously postulated.²⁶ Our impressions therefore stand in contrast to the observations of other authors who have described the hAM as being unsuitable for wound coverage because of its lack of mechanical stability.²⁷

With regard to the wound contraction, we expected less contraction in the groups treated with hAM compared with the control group. In contrast, the data showed that the membranes had no advantages with regard to contrac-

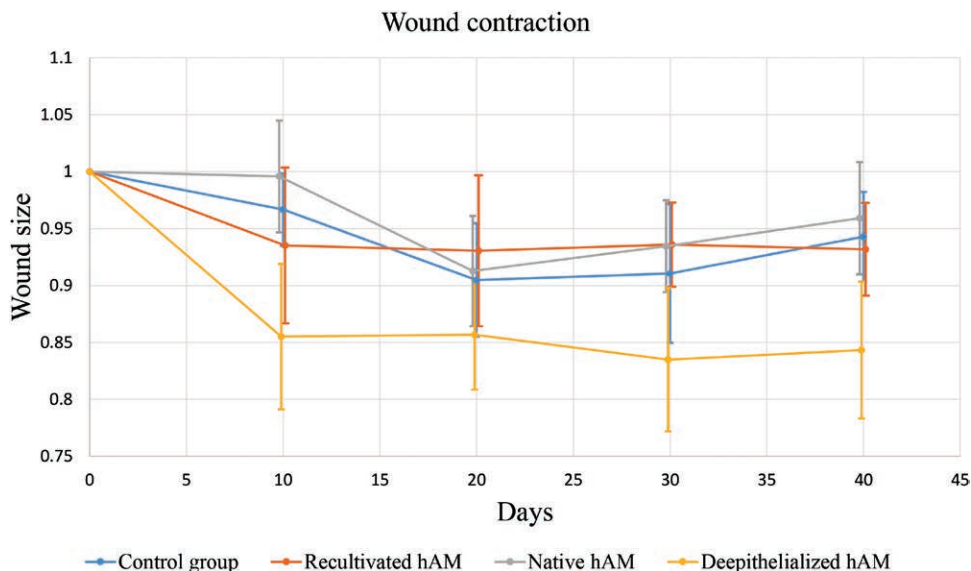


Fig. 5. Proportional wound sizes related to the initial size over time. Starting at day 0 (formation of the defect) and the related wound size (1), the groups showed various types of development regarding wound contraction. Wounds were examined every ten days till day 40. Mean values and SDs are demonstrated. A smaller wound size and therefore stronger wound contraction was observed for the rats treated with de-epithelialized hAM.

Table 2. VSS Score of the Various Groups and Univariate ANOVA

	Mean Value \pm SD	P Value of the Univariate ANOVA
Control group	5.33 \pm 1.03	$P = 0.46$
Recultivated hAM	4.83 \pm 0.75	
Native hAM	5.33 \pm 1.37	
De-epithelialized hAM	5.83 \pm 0.98	

The individual groups did not differ significantly regarding their score in the VSS ($P = 0.46$).

tion, with the de-epithelialized hAM exhibiting the most extent wound contraction (Table 1). As wound contraction is caused by activated myofibroblasts, which in turn are stimulated by mechanical factors and an increased release of TGF-beta, we expect complex cell–cell interactions that are as yet unknown to be the reason for our results.²⁸ In terms of the time course of the wound contraction, no faster or slower contractions between the groups were observed (Table 1, Fig. 5). Therefore, a significant influence on myofibroblasts activated by cytokines in the proliferation and granulation phase—within a reduced inflammatory reaction caused by anti-inflammatory agents of the hAM—seems unlikely.²⁹ The speed of the re-epithelialization was not examined in our study design.

The VSS is an established clinical scale. Other scales, which provide more extensive evidence, were unavailable for rats. Our measurements showed no significant differences between the groups (Table 2). Therefore, no significant effect of the hAM on macroscopic scar morphology is detectable, in contrast to the promoted wound healing properties.^{30,31}

The histological hematoxylin–eosin staining qualitatively showed no obvious differences between the groups with regard to the morphological properties of the scar. This suggests a low effect of the hAM on the final histology of the scar. The laminin staining revealed no consistent

basement membrane in the control group, such as that described by other research groups.³² Other researchers, however, have found laminin in full-thickness skin defects without skin replacement, but later over the time course of the wound healing than in wounds treated with hAM.²⁶ Therefore, the later formation of basement membrane in our control group cannot be ruled out. In contrast, all the rats treated with hAM showed consistent basement membranes (Fig. 7), as found elsewhere.²⁶ This indicates either an incorporation of the basement membrane of the hAM or an enhanced stimulation of the synthesis of a new basement membrane within accelerated wound healing. In any case, altered or missing basement membranes are described as being the cause of pathological scars such as keloids.³² Consequently, the formations of these pathological scars could be inhibited by the use of amniotic membranes as wound coverage for full-thickness skin defects. Similar observations were made by other research groups when hAM was used to cover split thickness skin defects.¹¹ To determine whether the hAM, and especially the basement membrane, becomes incorporated or substituted in the rat tissue, its structures should be bioorthogonal labeled, as previously presented for other tissues.³³ Additional research in larger groups should be performed to verify differences in the formation of the basement membrane.

This study presents some limitations that should be considered. The hAM exhibits variable interindividual conditions for reasons such as age, general condition, gestational age, and sex of the fetus that play significant roles in the expression of cytokines, hyaluronic acid, and other factors.³⁴ Moreover, intraindividual factors such as the sampling location are relevant. The hAM of the cervical zone is often thinner and has less epithelium than hAM sampled from other zones and the expression of cytokines also varies with location.³⁴ Additionally, the alignment of the collagen fibers of the hAM is irregular with occasional weak spots.³⁵ For logistical reason, we used cryoconserved hAM. Some authors have found low expression of An-

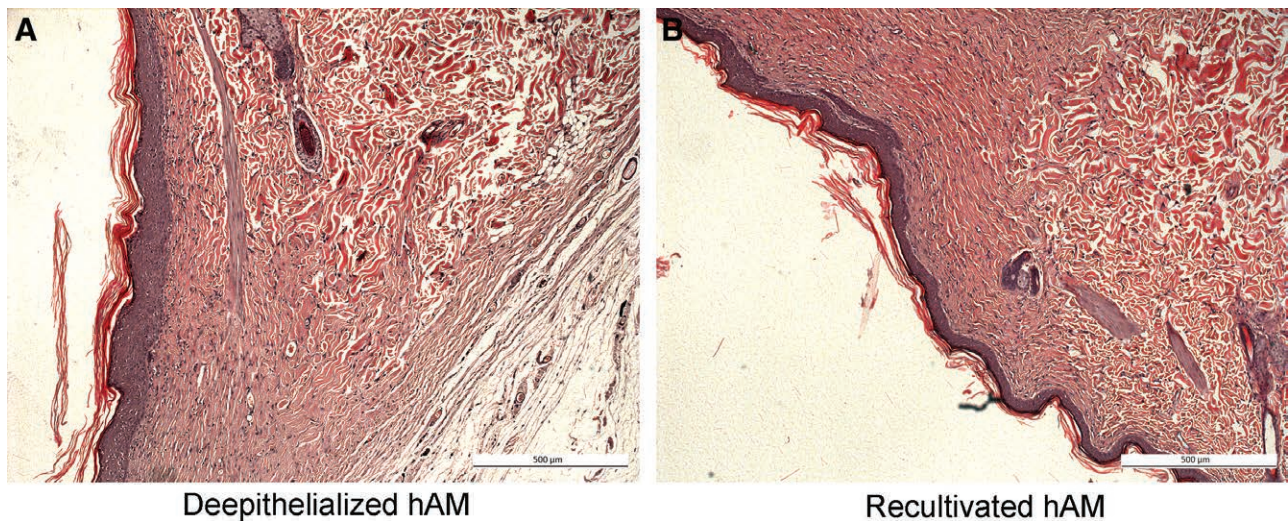


Fig. 6. Wound biopsies stained by hematoxylin–eosin. Transition from healthy to scar tissue. 25 \times . A and B, Two exemplary biopsies are displayed; clearly visible structural differences are present when passing from healthy to scar tissue. Skin appendages are lacking in the scar tissue, the connective tissue is dense and the epidermis is consistent and regularly formed.

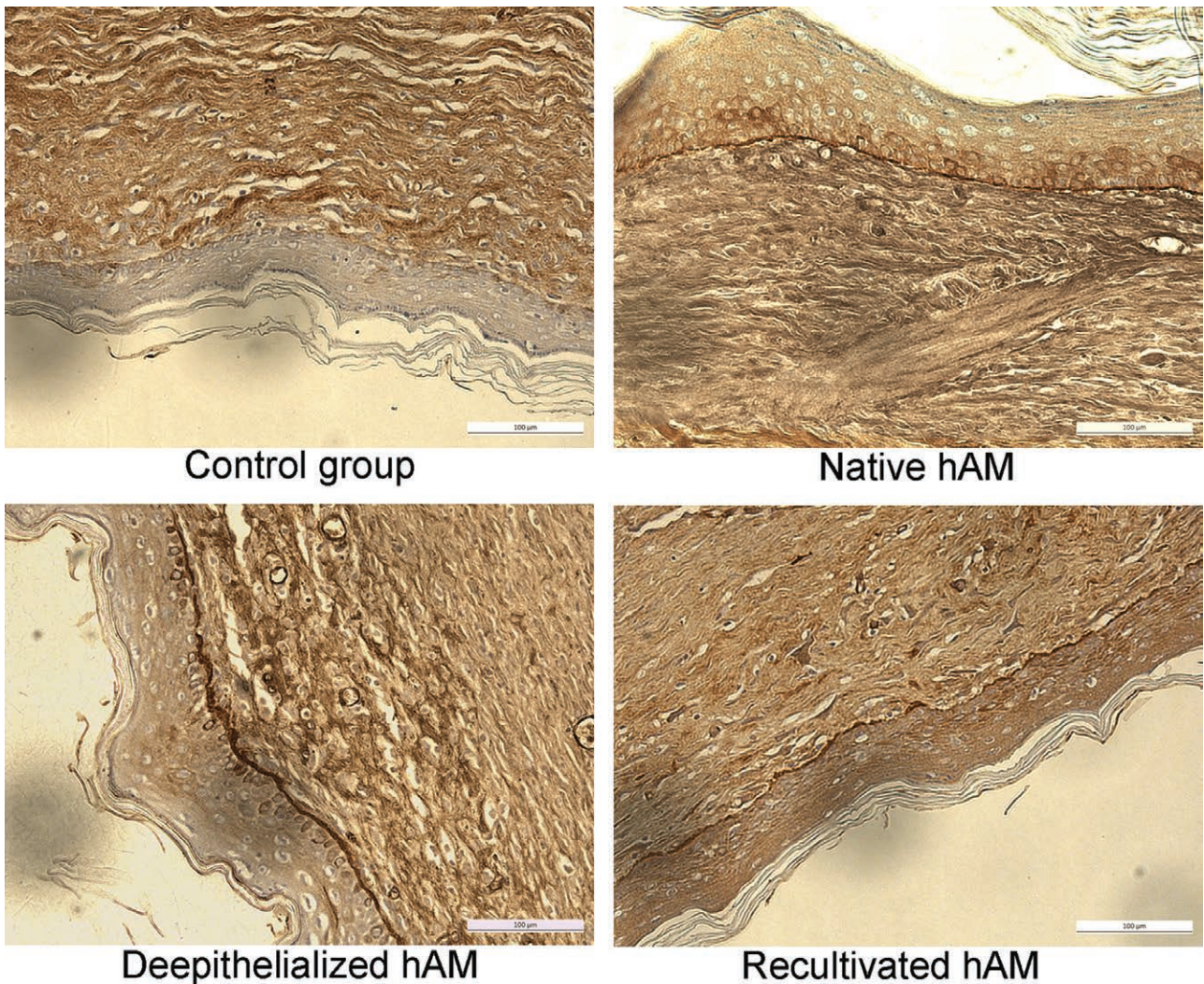


Fig. 7. Wound biopsies stained for Laminin. 100 \times . Laminin staining was performed to identify the basement membranes. Basement membranes were found in the rats treated with native, recultivated and especially de-epithelialized hAM. The control group showed no membrane.

giogenin, IL-6, and CP-1 in such processed membranes compared with fresh membranes,³⁶ whereas others have detected no differences.³⁷ The conservation of the hAM has possible harmful effects and should therefore be avoided in further studies.

A rat model is usually one of the first steps to evaluate a new wound treatment. However, rats are loose skinned and heal wounds primarily by contraction instead of granulation and re-epithelialization. Therefore, for further studies, a more humanized wound healing model should be evaluated such as mini pigs or splinted wounds in rats.³⁶

With regard to the removal of the dressing, the 10-day period seemed to be too long as, despite the fatty gauze and a cautious approach, adhesions occurred between the wound area and the dressing and ultimately led to traumatic wound reopening. In 2 cases, tissue that was possibly part of the amniotic membrane was found sticking to the dressing (Fig. 8). Although the use of a light pressure dressing is obligatory to minimize submembranous hema-

tomas and to reduce the risk of infections, the time during which the dressing is applied could be reduced to 7 days to adapt to general recommendations and more antiadhesive agents could be used.^{29,37}

Regarding the results of the scar appearance, some authors look critically at the evaluation of scars on the basis of existing scores altogether mentioning the low test quality and the few test items.²³ Therefore, the results of the VSS should be interpreted with caution.

Finally, a more profound histological evaluation with the use of further immunohistochemical studies and (semi)quantitative methods to describe the morphologic qualities of the scar should be performed in further research.

CONCLUSIONS

With regard to wound contraction and scar appearance, we could find no advantages for skin defects treated

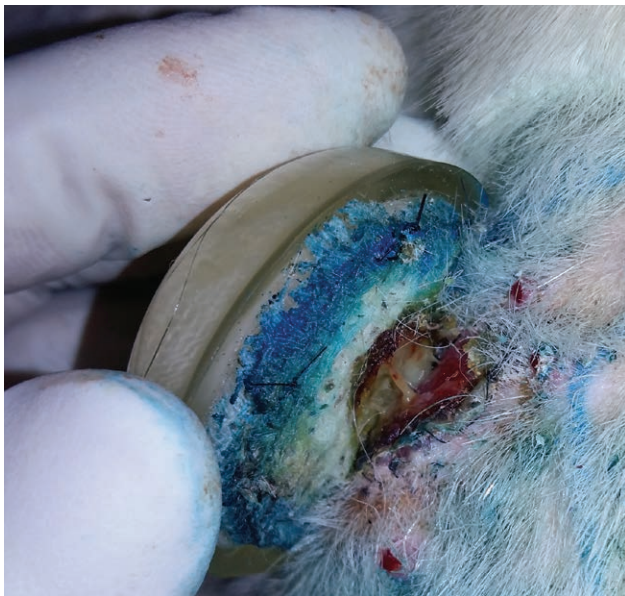


Fig. 8. Removal of the dressing with wound reopening. Removal of the dressing in this example led to the reopening of the wound area. Tissue that might have been part of the hAM (arrow) had stuck to the dressing.

with hAM. Histologically, rats treated with membranes qualitatively showed no difference in morphology of the scar, but consistent basement membranes as opposed to the control group, which showed no basement membranes at all. This interesting aspect should be investigated further for its possible effect in the prevention of pathological scars. Several limiting factors should also be addressed in further research.

Samuel John, MD

Ernst-Zielinski-Straße 12

07745 Jena, Germany

E-mail: Samuel_john@web.de

REFERENCES

1. Presland RB, Jurevic RJ. Making sense of the epithelial barrier: what molecular biology and genetics tell us about the functions of oral mucosal and epidermal tissues. *J Dent Educ.* 2002;66:564–574.
2. Xiao-Wu W, Herndon DN, Spies M, et al. Effects of delayed wound excision and grafting in severely burned children. *Arch Surg.* 2002;137:1049–1154.
3. Prasanna M, Mishra P, Thomas C. Delayed primary closure of the burn wounds. *Burns.* 2004;30:169–175.
4. Rhee PH, Friedman CD, Ridge JA, et al. The use of processed allograft dermal matrix for intraoral resurfacing: an alternative to split-thickness skin grafts. *Arch Otolaryngol Head Neck Surg.* 1998;124:1201–1204.
5. Zelen CM, Serena TE, Denoziere G, et al. A prospective randomised comparative parallel study of amniotic membrane wound graft in the management of diabetic foot ulcers. *Int Wound J.* 2013;10:502–507.
6. Rosenberg AS, Munitz TI, Maniero TG, et al. Cellular basis of skin allograft rejection across a class I major histocompatibility barrier in mice depleted of CD8+ T cells in vivo. *J Exp Med.* 1991;173:1463–1471.
7. Tomasek JJ, Gabbiani G, Hinz B, et al. Myofibroblasts and mechano-regulation of connective tissue remodelling. *Nat Rev Mol Cell Biol.* 2002;3:349–363.
8. Moore P, Moore M, Blakeney P, et al. Competence and physical impairment of pediatric survivors of burns of more than 80% total body surface area. *J Burn Care Rehabil.* 1996;17(6 pt 1):547–551.
9. Tanaka A, Hatoko M, Tada H, et al. An evaluation of functional improvement following surgical corrections of severe burn scar contracture in the axilla. *Burns.* 2003;29:153–157.
10. MacNeil S. Progress and opportunities for tissue-engineered skin. *Nature.* 2007;445:874–880.
11. Loeffelbein DJ, Rohleder NH, Eddicks M, et al. Evaluation of human amniotic membrane as a wound dressing for split-thickness skin-graft donor sites. *Biomed Res Int.* 2014;2014:572183.
12. McKenna B, Summers NJ. Amnion: the ideal scaffold for treating full-thickness wounds of the lower extremity. *Clin Podiatr Med Surg.* 2018;35:1–9.
13. Kogan S, Sood A, Granick MS. Amniotic membrane adjuncts and clinical applications in wound healing: a review of the literature. *Wounds.* 2018;30:168–173.
14. Campelo MBD, Santos JAF, Maia Filho ALM, et al. Effects of the application of the amniotic membrane in the healing process of skin wounds in rats. *Acta Cir Bras.* 2018;33:144–155.
15. Muller L, Brighton LE, Carson JL, et al. Culturing of human nasal epithelial cells at the air liquid interface. *J Vis Exp.* 2013.
16. Kubota Y, Kleinman HK, Martin GR, et al. Role of laminin and basement membrane in the morphological differentiation of human endothelial cells into capillary-like structures. *J Cell Biol.* 1988;107:1589–1598.
17. LeBleu VS, Macdonald B, Kalluri R. Structure and function of basement membranes. *Exp Biol Med (Maywood).* 2007;232:1121–1129.
18. Wood FM, Stoner M. Implication of basement membrane development on the underlying scar in partial-thickness burn injury. *Burns.* 1996;22:459–462.
19. John S, Kesting MR, Paulitschke P, et al. Development of a tissue-engineered skin substitute on a base of human amniotic membrane. *J Tissue Eng.* 2019;10:2041731418825378.
20. Ahn KM, Lee JH, Hwang SJ, et al. Fabrication of myomucosal flap using tissue-engineered bioartificial mucosa constructed with oral keratinocytes cultured on amniotic membrane. *Artif Organs.* 2006;30:411–423.
21. Mariappan I, Maddileti S, Savy S, et al. In vitro culture and expansion of human limbal epithelial cells. *Nat Protoc.* 2010;5:1470–1479.
22. Lin H, Li H, Cho HJ, et al. Air-liquid interface (ALI) culture of human bronchial epithelial cell monolayers as an in vitro model for airway drug transport studies. *J Pharm Sci.* 2007;96:341–350.
23. Tyack Z, Simons M, Spinks A, et al. A systematic review of the quality of burn scar rating scales for clinical and research use. *Burns.* 2012;38:6–18.
24. Cardiff RD, Miller CH, Munn RJ. Manual hematoxylin and eosin staining of mouse tissue sections. *Cold Spring Harb Protoc.* 2014;2014:655–658.
25. Gupta A, Kumar P. Assessment of the histological state of the healing wound. *Plast Reconstr Surg.* 2015;2:239–242.
26. Loeffelbein DJ, Baumann C, Stoeckelhuber M, et al. Amniotic membrane as part of a skin substitute for full-thickness wounds: an experimental evaluation in a porcine model. *J Biomed Mater Res B Appl Biomater.* 2012;100:1245–1256.
27. Murphy SV, Skardal A, Song L, et al. Solubilized amnion membrane hyaluronic acid hydrogel accelerates full-thickness wound healing. *Stem Cells Transl Med.* 2017;6:2020–2032.

28. Fritsch PO. *Dermatologie Venerologie*. 2nd ed. Heidelberg, Germany: Springer-Verlag; 2004.
29. Hoffmann TK, Arnolds J, Schuler PJ, et al. Secondary wound healing. Effective treatment concept after basal cell carcinoma resection in the central midface. *HNO*. 2012;60:605–610.
30. Jiang D, Liang J, Noble PW. Hyaluronan in tissue injury and repair. *Annu Rev Cell Dev Biol*. 2007;23:435–461.
31. Meinert M, Eriksen GV, Petersen AC, et al. Proteoglycans and hyaluronan in human fetal membranes. *Am J Obstet Gynecol*. 2001;184:679–685.
32. Yang S, Sun Y, Geng Z, et al. Abnormalities in the basement membrane structure promote basal keratinocytes in the epidermis of hypertrophic scars to adopt a proliferative phenotype. *Int J Mol Med*. 2016;37:1263–1273.
33. Wei L, Hu F, Chen Z, et al. Live-cell bioorthogonal chemical imaging: stimulated raman scattering microscopy of vibrational probes. *Acc Chem Res*. 2016;49:1494–1502.
34. Litwiniuk M, Grzela T. Amniotic membrane: new concepts for an old dressing. *Wound Repair Regen*. 2014;22:451–456.
35. Schmidt W, Klima G. Experimental and histologic studies on fetal membrane tensility and membrane rupture. *Zentralbl Gynakol*. 1989;111:129–141.
36. Galiano RD, Michaels JV, Dobryansky M, et al. Quantitative and reproducible murine model of excisional wound healing. *Wound Repair Regen*. 2004;12:485–492.
37. Maral T, Borman H, Arslan H, et al. Effectiveness of human amnion preserved long-term in glycerol as a temporary biological dressing. *Burns*. 1999;25:625–635.